Open Access

Effect of Iron Doping on the Electron Density Distribution in Pure Aluminium

R. Saravanan* and M. Prema Rani

Department of Physics, The Madura College, Madurai – 625 011, Tamil Nadu, India

Abstract: The electronic structure of pure and doped aluminium with dilute amounts of iron impurities (0.215 wt % Fe and 0.304 wt % Fe) has been analyzed using reported X-ray data sets and the MEM (maximum entropy method) technique. Qualitative as well as quantitative assessment of the electron density distribution in these samples has been made. The mid-bond characterization leads to a conclusion about the nature of doping of impurities. An expansion of size of the atoms is observed with the addition of Fe impurities.

1. INTRODUCTION

The analysis of bonding and electronic structure of metals is useful because of the variety of applications of metals, particularly when they are doped with other elements. There has been tremendous impetus in the study of electronic structure of solids, both theoretically and experimentally because of the necessity. When the system is dilute doped, it is possible to study only the average electronic structure. But, when suitable tools like MEM technique are available, they can be effectively used, to elucidate the fine features of bonding as has been tried in the present work. Fourier synthesis of electron densities can be of useful in picturising the bonding between two atoms, but, it suffers from the major disadvantage of series termination error and negative electron densities that prevent the clear understanding of the fine nature of bonding between atoms, the factor which has been intended to be analyzed. The advent of MEM (Maximum Entropy Method) solves many of these problems. MEM electron densities are always positive and even with limited number of data, one can determine reliable electron densities resembling true densities. In this work, such an analysis also has been carried out using the formalism of Collins [1] using the datasets reported by Mohanlal and Pathinettam Padiyan [2].

In our series of research studies on the bonding in materials, we have analyzed LiF, NaF, GaAs, CdTe and some oxides (Israel *et al.* [3,4], Saravanan *et al.* [5], Kajitani *et al.* [6]) using MEM technique and reported X-ray data and obtained precise information on the bonding in the above materials. The nature of bonding in these materials as analyzed are found to be ionic, mixed covalent and ionic, and 'oxide' bonding.

In the present study on aluminium with iron impurities, we have attempted to study the metal bonding and to bring out the details of doping using MEM technique. The X-ray structure factor data sets have been taken from Mohanlal and Pathinettam Padiyan [2] who have reported precise structure factors collected from a home-built manual X-ray diffractometer. Data sets for pure aluminium, Al + 0.189 wt % Fe, Al + 0.215 wt % Fe and Al + 0.304 wt % Fe are available from this report [2]. Other relevant details can be found from this paper. Among these data sets, one corresponding to Al + 0.189 wt % Fe has been excluded from the present analysis after examining the preliminary results from MEM and multipole methods (the low doping level does not allow any meaningful conclusions of the obtained results). The remaining three data sets, i.e., those of pure aluminium, Al + 0.215 wt % Fe and Al + 0.304 wt % Fe were used in this study. It was observed that the B_{eff} and the expected number of vacant sites in Al + 0.215 wt % Fe are much better than those in Al + 0.189 wt % Fe, though slight variations of these quantities is observed, compared to pure aluminium and Al + 0.304 wt % Fe (it has been reported [2] that the number of vacant sites created in the Al lattice increases with the number of Fe impurities and in the case of Al + 0.189 wt % Fe, less vacancies are created than that expected). Hence, data set for Al + 0.215 wt % Fe has been included in the present analysis in order to have a composition of iron in between pure aluminium and Al + 0.304 wt % Fe and to compare the results.

2. DATA ANALYSIS

All the reported data sets have been analyzed using JANA 2000 [7] software package. The refined structure factors were used for the MEM refinements of the electron densities. The characteristics of the structural refinements are given in Table **1**. The reliability indices (R-factors) and the matching of thermal parameters (B) with the corresponding reported values for all three crystal structures indicate that the quality of the experimental data is suitable enough for the electron density analysis. The same number of data for all three compositions samples has been utilized for the present analysis in order to make a comparison of the results.

The MEM analysis has been carried out as outlined in our earlier papers (Israel *et al.* [3, 4], Saravanan *et al.* [5], Kajitani *et al.* [6]). The cell was divided into 128^3 pixels. For the numerical MEM computations, the software package PRIMA [8] was used. For the 2D and 3D representation of the electron densities, the program VESTA [9] package was used. In all three cases, the convergence condition C = 1.0,

*Address correspondence to this author at the Department of Physics, The Madura College, Madurai – 625 011, Tamil Nadu, India; Tel: +91-452-2673354; Ext: 211; +91-94430 69852;
E-mail: saragow@dataone.in, website: www.saraxraygroup.net

1874-8465/09 2009 Bentham Open

was obtained after several cycles of the MEM refinement. The main characteristics of the refinements are listed in Table **2**. The reliability indices are found to be very low. To analyze the MEM results, one-dimensional profiles along different directions of the unit cell and two-dimensional electron density contour maps have been constructed. The results of the 1-D analysis have given in Table **3**. The three dimensional electron density superimposed with the structural model of aluminium is shown for three compositions in Figs. (**1 a-c**) respectively. The 2-D electron density contour maps drawn on (100) plane are given in Figs. (**2 a-c**). Figs. (**3 a-c**) represent the 2-D maps on the (110) plane. The 1-D variation of the electron density is shown in Figs. (**4 a-c**). Fig. (**4a**) represents the variation along the [100] direction for all three compositions, Fig. (**4b**) that along the [110] direction and Fig. (**4c**) along the [111] direction. The analysis on the MEM results is given in the next section.

Table 1. Structure Refinements

Sample	a_0 (Å)	Number of Reflections	B* (Å^2)	R(%)	*w*R(%)
Al	4.0440	18	0.825(0.069)	2.22	2.82
Al+0.215%Fe	4.0501	18	1.038(0.061)	2.61	2.86
Al+0.304%Fe	4.0452	18	1.442(0.053)	2.61	2.82

* Debye-Waller factor.

Table 2. The MEM Refinements

Sample	a_0 (Å)	Number of Reflections	Cycles	R(%)	*w*R(%)	Lagrange Parameter (λ)	Resolution of the Map (Å/pixel)
Al	4.0440	18	713	0.2276	0.2867	0.010	0.0316
Al+0.215%Fe	4.0501	18	832	0.2939	0.2969	0.012	0.0316
Al+0.304%Fe	4.0452	18	5703	0.2673	0.3189	0.012	0.0316

Table 3. Maxima of the MEM Electron Density Revealed in Different 1-D Sections of a Unit Cell for the Different Compositions

	Direction					
	[100]		[110]		[111]	
Composition	Position (Å)	E.D. (e/Å^3)	Position (Å)	E.D. (e/Å^3)	Position (Å)	E.D (e/Å^3)
Al	0.000*	128.75	0.000*	128.75	0.000*	128.75
	1.485	0.14	1.429	0.22	1.477	0.15
	2.022	0.19	1.698	0.20	1.751	0.15
Al+0.215%Fe	0.000*	109.21	0.000*	109.21	0.000*	109.21
	1.455	0.14	1.298	0.19	1.534	0.15
	2.025	0.19	1.432	0.19	1.753	0.15
					2.631	0.12
					3.508	0.19
					4.384	0.12
					5.261	0.15
Al+0.304%Fe	0.000*	85.79	0.000*	85.79	0.000*	85.79
	1.517	0.12	1.430	0.15	1.752	0.11
	2.022	0.15			2.080	0.11
					2.682	0.09
					3.503	0.15
					4.324	0.09
					5.254	0.11

* At origin

E.D. Electron Density.

3. RESULTS AND DISCUSSION

As expected from the substitution Al by Fe, the peak density decreases with the increase of Fe impurity (Fig. **4**). As more and more Fe atoms occupy the host aluminium lattice substitutionally, the size of the charge cloud increases due to the larger atomic radius of iron (1.72 Å - for aluminium, the atomic radius is 1.43 Å). The electron density be-

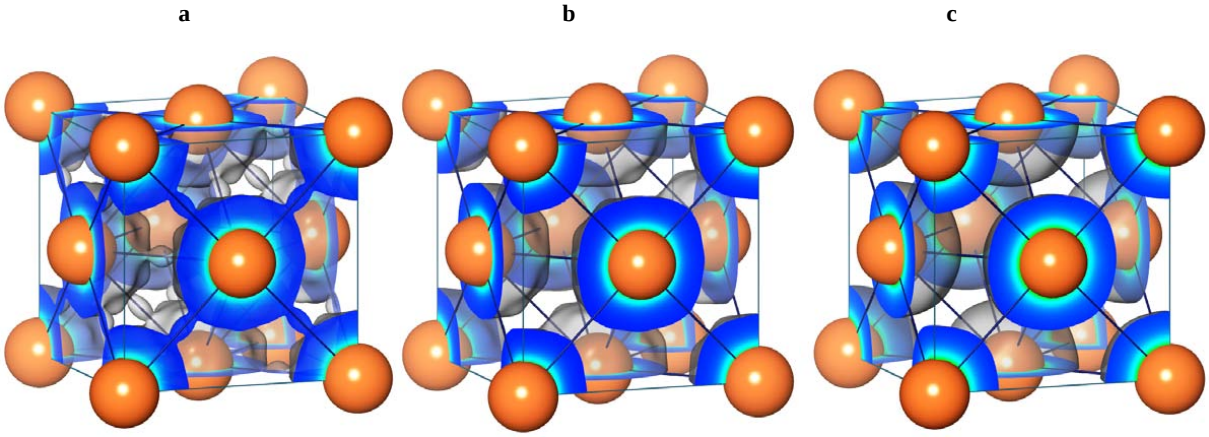

Fig. 1(a). Three dimensional representation of the electron density of pure aluminium super imposed with the structural model. Iso-surface level is 0.2. (**b**) Three dimensional representation of the electron density of Al + 0.215 % Fe super imposed with the structural model. Iso-surface level is 0.2. (**c**) Three dimensional representation of the electron density of Al + 0.304 % Fe super imposed with the structural model. Iso-surface level is 0.2.

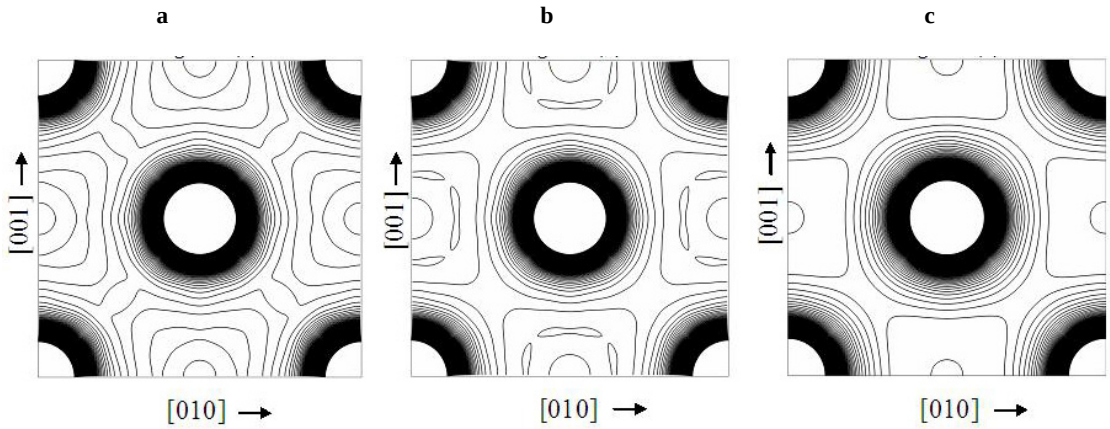

Fig. 2(a). MEM electron density distribution of pure aluminium on the (100) plane. Contour range is from 0.0 to 5.0 e/Å^3. Contour interval is 0.03 e/Å^3. (**b**) MEM electron density distribution of Al + 0.215 % Fe on the (100) plane. Contour range is from 0.0 to 5.0 e/Å^3. Contour interval is 0.03 e/Å^3. (**c**) MEM electron density distribution of Al + 0.304 % Fe on the (100) plane. Contour range is from 0.0 to 5.0 e/Å^3. Contour interval is 0.03 e/Å^3.

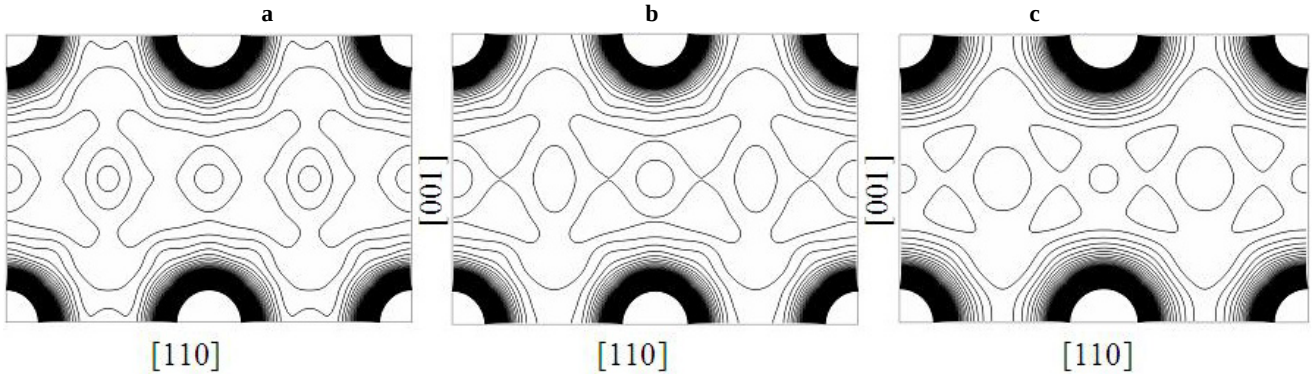

Fig. 3(a). MEM electron density distribution of pure aluminium on the (110) plane. Contour range is from 0.0 to 5.0 e/Å^3. Contour interval is 0.03 e/Å^3. (**b**) MEM electron density distribution of Al + 0.215 % Fe on the (110) plane. Contour range is from 0.0 to 5.0 e/Å^3. Contour interval is 0.03 e/Å^3. (**c**) MEM electron density distribution of Al + 0.304 % Fe on the (110) plane. Contour range is from 0.0 to 5.0 e/Å^3. Contour interval is 0.03 e/Å^3.

tween atoms along the [110] direction also decreases with impurities (Table **3** and Fig. (**3b**)) though it is almost a constant along the other two directions, the [100] and [111] (Table **3**). The bonding direction shows (which is [110] direction, because the first nearest neighbors are along this direction), that the mid-bond electron density also decreases with the addition of Fe impurities as shown in the insert of Fig. (**4b**). The mid-bond density along the other two directions, the [100] and [111] (inserts of Figs. (**4a**) and (**4c**)), does not reveal any trend with the Fe impurities, because the values of the densities involved are very low along these non-bonding directions and the humps seen in inserts of Figs. (**4a**) and (**4c**) are due to the interference of the electron density of the

a

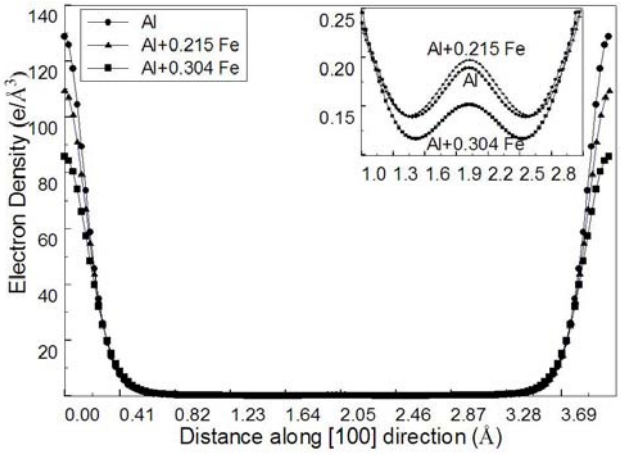

Fig. 4(a). One-dimensional MEM low-electron density profiles of pure aluminium, Al + 0.215 % Fe and Al + 0.304 % Fe along the [100] direction. The mid-bond variation of the electron density is shown as insert, in which the y-axis represents the electron density in e/Å^3 and the x-axis, the distance along the [100] direction in Å.

b

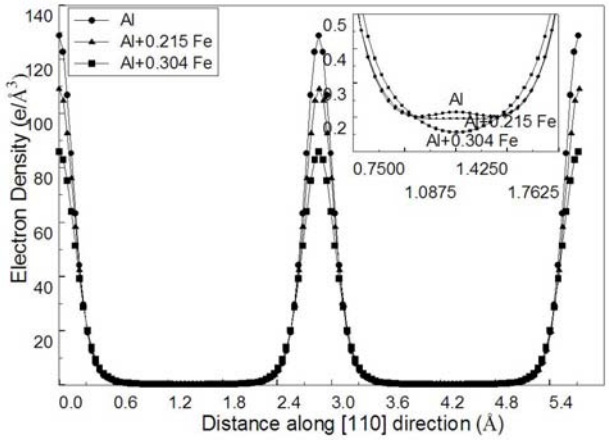

Fig. 4(b). One-dimensional MEM low-electron density profiles of pure aluminium, Al + 0.215 % Fe and Al + 0.304 % Fe along the [110] direction. The mid-bond variation of the electron density is shown as insert, in which the y-axis represents the electron density in e/Å^3 and the x-axis, the distance along the [110] direction in Å.

FCC atoms in the unit cell (NNM - Non Nuclear Maxima, along the non-bonding directions). The MEM electron density distribution of pure Al, Al + 0.215 % Fe and Al + 0.304 % Fe on the (100) plane (Figs. (**2 a**-**c**)) shows clear densities with very low noise levels. The large thermal vibration and smearing of charges is seen. Hence the increased size of the electronic clouds can be attributed to the static and dynamic thermal vibration parameters and also to the increased host lattice substitution of the Fe atoms.

c

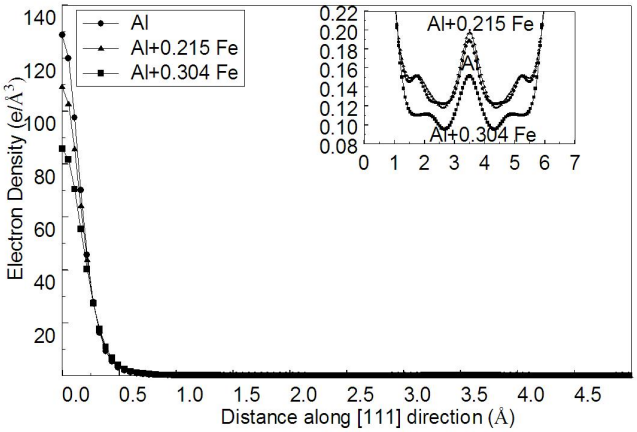

Fig. 4(c). One-dimensional MEM low-electron density profiles of pure aluminium, Al + 0.215 % Fe and Al + 0.304 % Fe along the [111] direction. The mid-bond variation of the electron density is shown as insert, in which the y-axis represents the electron density in e/Å^3 and the x-axis, the distance along the [111] direction in Å.

4. CONCLUSION

The electron density distribution in the unit cell of Al with different iron impurity has been studied precisely using currently available most versatile technique, the MEM analysis of the electron densities. Minute changes in the density details and the incorporation of impurities in the host lattice have been revealed. The electron density and the mid-bond electron density decrease with more Fe impurity doping as evidenced from the 1D electron densities. Hence, the bonding strength in Al decreases with Fe addition. In addition to the electron density details showing up themselves as actual distributions of atomic electrons, the thermal parameters also show a similar trend with respect to impurity addition. Moreover, an increase in the atomic sizes with the addition of more Fe impurities is observed pictorially as revealed by the 2D electron densities in Fig. (**2**). Since, the crystallographic system presently studied is highly symmetric, there are no appreciable shift/changes in the mid-bond positions despite the increase in the atomic sizes with more addition of Fe impurities.

REFERENCES

[1] Collins DM. Electron density images from imperfect data by interactive entropy maximization. Nature 1982; 298: 49.

[2] Mohanlal SK, Pathinettam Padiyan D. An X-ray study of defect structure of Al with Fe impurities. Cryst Latt Def Amorph Mater 1987; 14: 23.

[3] Israel S, Saravanan R, Srinivasan N, Mohanlal SK. An Investigation on the bonding in MgO, CaO, SrO and BaO from the MEM electron density distributions. J Phys Chem Solids 2003; 64: 879.

[4] Israel S, Saravanan R, Srinivasan Rajaram RK. High resolution electron density mapping for LiF and NaF by Maximum Entropy Method (MEM). J Phys Chem Solids 2002; 64/1: 43.

[5] Saravanan R, Ono Y, Isshiki M, Ohno K, Kajitani T. Electron density distribution in GaAs using MEM. J Phys Chem Solids 2002; 64/1: 51-8.

[6] Kajitani T, Saravanan R, Ono Y, Ohno K, Isshiki M. High resolution electron density distribution determination for GaAs and CdTe. J Cryst Growth 2001; 229: 130-6.

[7] Petříček V. Dušek M, Palatinus L. JANA 2000, The crystallographic computing system. Institute of Physics, Academy of sciences of the Czech republic, Praha 2000.

[8] Izumi F, Dilanian RA. Recent Research Developments in Physics, Part II, Transworld Research Network, Trivandrum 2002; Vol. 3, pp. 699–726.

[9] Momma K, Izumi F. Commission on Crystallographic. Computing IUCr. Newslett 2006; 7: 106.

Received: April 23, 2008 Revised: December 16, 2008 Accepted: December 16, 2008

© Saravanan and Rani; Licensee *Bentham Open*.

This is an open access article licensed under the terms of the Creative Commons Attribution Non-Commercial License (http://creativecommons.org/licenses/by-nc/3.0/) which permits unrestricted, non-commercial use, distribution and reproduction in any medium, provided the work is properly cited.